

Nanoscale

Accepted Manuscript



This is an *Accepted Manuscript*, which has been through the Royal Society of Chemistry peer review process and has been accepted for publication.

Accepted Manuscripts are published online shortly after acceptance, before technical editing, formatting and proof reading. Using this free service, authors can make their results available to the community, in citable form, before we publish the edited article. We will replace this *Accepted Manuscript* with the edited and formatted *Advance Article* as soon as it is available.

You can find more information about *Accepted Manuscripts* in the [Information for Authors](#).

Please note that technical editing may introduce minor changes to the text and/or graphics, which may alter content. The journal's standard [Terms & Conditions](#) and the [Ethical guidelines](#) still apply. In no event shall the Royal Society of Chemistry be held responsible for any errors or omissions in this *Accepted Manuscript* or any consequences arising from the use of any information it contains.

Cite this: DOI: 10.1039/c0xx00000x

www.rsc.org/xxxxxx

ARTICLE TYPE**Nanostructured Carbon Materials Based Electrothermal Air Pump Actuators**Qing Liu^{a,b}, Luqi Liu^{*a}, Jun Kuang^{a,b}, Zhaohe Dai^{a,b}, Jinhua Han^{a,b}, Zhong Zhang^{*a}

Received (in XXX, XXX) Xth XXXXXXXXX 20XX, Accepted Xth XXXXXXXXX 20XX

DOI: 10.1039/b000000x

5 Actuator materials can directly convert different types of energy into mechanical energy. In this work, we designed and fabricated electrothermal air pump-type actuators by utilization of various nanostructured carbon materials, including single wall carbon nanotubes (SWCNT), reduced graphene oxide (*r*-GO), and graphene oxide (GO)/SWCNT hybrid films as heating elements to transfer electrical stimulus into thermal energy, and finally convert it into mechanical energy. Both the actuation displacement and working

10 temperature of the actuator films show the monotonically increasing trend with increasing the driving voltages within the actuation process. Compared with common polymer nanocomposites based electrothermal actuators, our actuators performed better actuation performances with low driving voltages (<10 V), large generated stress (tens of MPa), high gravimetric density (tens of J/kg), and short response time (few hundreds of milliseconds). Besides that, the pump actuators exhibited excellent stability under

15 cyclic actuation tests. Among these actuators, relatively larger actuation strain was obtained for the *r*-GO film actuator due to the intrinsic gas-impermeability nature of graphene platelets. In addition, the high modulus of the *r*-GO and GO/SWCNT films also guaranteed the large generated stress and high work density. Specifically, the generated stress and gravimetric work density of the GO/SWCNT hybrid film actuator could reach up to more than 50 MPa and 30 J/kg, respectively, under a driving voltage of 10 V.

20 The resulting stress value is at least two orders of magnitude higher than that of natural muscles (~0.4 MPa).

Introduction

Actuator materials that can directly convert various energies to mechanical energy have shown great potentials in artificial

25 muscles, robotics and biomedical fields.¹⁻⁵ Among them, electroactive polymers (EAPs) have attracted great attention in recent decades due to the merits of lightweight, high flexibility, and large actuation strain in response to electrical stimulation.² Determined by the actuation mechanisms, EAPs based actuators

30 can be broadly divided into two categories: ionic and electric-field driven EAPs. In the ionic classification, the EAPs (*e.g.* conducting polymers, ionic polymer metal composites) are mostly actuated under relatively lower driving voltage, but the harsh working environment (electrolyte solutions or certain

35 environment humidity) severely restricts their broad applications.^{6, 7} In the meantime, electronic EAPs (including elastomers and dielectric polymers *etc*) can work in air and exhibit large actuation strain, quick response in the order of millisecond, and high energy densities. However, owing to low

40 dielectric constants relative to ceramics, high electrical fields (as high as 1.3×10^8 V/m) are generally required and the force output are relatively low, which further challenges widespread utilizations.^{8, 9} Recently, the reduced electric-fields by up to two orders of magnitude were realized in various polymer systems

45 through inclusion of CNT additives.^{10, 11} To further reduce the magnitude of electric field required to induce actuation, polymer

nanocomposite electrothermal actuators, such as CNT/polydimethylsiloxane (PDMS) and conductive carbon nanoparticles/Nafion composites were developed.¹²⁻¹⁴ In such

50 cases, the electric field could be reduced to as low as $\sim 1.5 \times 10^3$ V/m. The actuation mechanism is attributed to thermal expansion of the polymers resulting from Joule heating once an external voltage is applied to the samples. In general, elastomers and soft materials with large thermal expansion coefficient will exhibit

55 large actuation strains. However, there are still a few drawbacks for the applications of such kinds of nanocomposite electrothermal actuators, particular for soft material based nanocomposites, as summarized below: (1) the force output greatly depends on the tensile modulus of polymer matrix, and a

60 low force output was observed for rubbery based nanocomposites; (2) the relative long response time on the level of seconds; (3) the polymer matrix would be degraded due to the heat generated by the electric current, and then lead to deterioration of the actuation performances. Later, Vaia *et al*

65 proposed to utilize CNT based thermoplastic polyimide nanocomposites as electrothermal actuator material to improve force output and thermal stability of actuator materials.¹⁵ However, owing to relatively high material stiffness (~2.5 GPa) and low conductivity (0.02 S/cm), the high driving voltages up to

70 1000 V and electric field $\sim 3.6 \times 10^4$ V/m were required to drive the actuators.

To realize low driving voltages while maintain large force output and thermal stability of electrothermal actuator materials,

in this work, we designed and fabricated an air pump-type

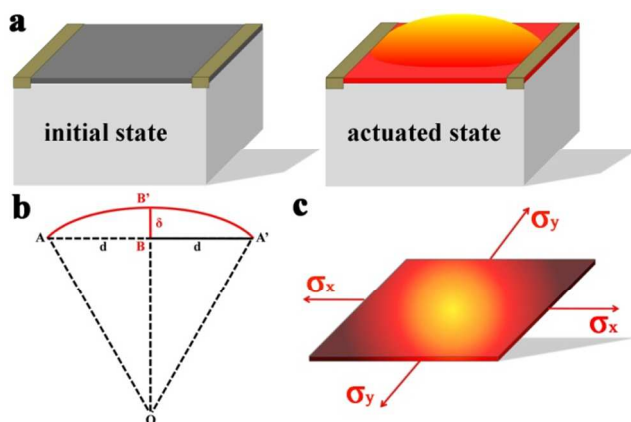


Figure 1 (a) Depiction of the initial and actuated state of air pump-type electrothermal actuator; (b) strain calculation depiction; (c) stress condition of the carbon material film under actuated state.

electrothermal actuator by utilizing nanostructured carbon materials including SWCNT and graphene as building and heating elements. The actuation mechanism of the air pump-type electrothermal actuator is based on the volume expansion of entrapped air once an electric current flows through the materials. According to the mechanism, gas-impermeability of the actuator material against air diffusion is required to maximize the actuation performance. It has been reported that graphene and GO platelets could act as perfect two dimensional gas-barriers against diffusion of liquids, vapours and gases, and thus air permeation and leakage during the actuation process could be hindered effectively.¹⁶⁻¹⁸ Besides that, earlier works have demonstrated that free-stranding nanostructured carbon material films (such as SWCNT, graphene and GO/CNT hybrid films) possess good electric conductivities, high tensile modulus, and thermal stability.¹⁹⁻²² Consequently, low driving voltage, large force outputs are expected for the air pump electrothermal actuators by employing various nanostructured carbon material films as actuator materials. Experimental results demonstrated that the generated stress for GO/SWCNT hybrid film actuators could reach up to 50 MPa at a 10 V driving voltage, which is at least two orders of magnitude higher than that of CNT/PDMS nanocomposite electrothermal actuators.¹⁴ Moreover, in contrast to thermal bimorph actuators composed by two materials with different thermal expansion coefficients,²³ our air pump-type actuator is simple to design and fabricate in lab and no micro-processing is demanded. Our work will be helpful not only to guide the design and fabrication of new-style actuators based on various nanostructured carbon materials, but also to deeply understand the microstructures influence of materials on actuation performances for air pump-type electromechanical actuators.

Experimental section

SWCNT (purity >95%, average diameter <1.6 nm) were purchased from Chengdu Organic Chemical Co. Ltd. For the SWCNT dispersion, 30 mg SWCNT was mixed with 600 mg Triton X-100 and 100 ml DI water, then subjected to ultrasonication for 20 minutes under 400W power in an ice bath (2 s on and 2 s off), the mixture was then centrifuged to remove

the aggregates (4500 rpm for 30 min). The supernatant dispersion was collected and utilized as starting material to prepare pure SWCNT films. GO was prepared from purified natural graphite by modified Hummers method according to previous study.²⁴ The obtained GO solution was diluted to 0.2mg/ml for the film preparation. For the GO/SWCNT hybrid solution preparation, 5 mg SWCNT and 100 mg Triton X-100 were firstly added into 100ml GO solution (0.2 mg/ml), and then the mixture was conducted to ultrasonication and centrifugation to get the final homogeneous supernatant. The SWCNT, GO and GO/SWCNT films were prepared by filtrating 20 ml solution through a cellulose membrane filter (47 mm in diameter, 0.22 μm pore size), respectively. For SWCNT and GO/SWCNT films filtration, 300 ml DI water was used to remove the surfactant. After air drying, the resulting films were peeled off from the membranes. The SWCNT and GO/SWCNT films were used as prepared without any further treatment while GO films were reduced referred Cheng's work by utilizing hydroiodic acid (HI) as reducing agent.²⁵ To avoid the damage of *r*-GO films during the reduction process, HI vapour was used instead of HI solution. After reduction, the *r*-GO films were washed with DI water and ethanol to remove the residue HI and I₂. The density of different carbon material films were measured by using weighing method and the final results were 0.9, 2.0, 1.5 × 10³ kg/m³ for SWCNT, *r*-GO, GO/SWCNT, respectively.

The morphology of as-prepared SWCNT, GO, *r*-GO and GO/SWCNT films was studied by Scanning Electron Microscope (SEM, HITACHI S-4800). A dynamic mechanical analyzer (TA, DMA Q800) were employed to evaluate the mechanical properties of the resulting films. The films were cut into strips with width of 2 mm, and the gauge length was controlled to be 10.0 ± 0.5 mm. The static tensile tests were conducted in displacement ramp mode with a pre-strain 0.01% and a ramp rate 20 μm/min. At least 5 samples were tested. The electrical property was tested using a Keithley 4200 instrument by the 4-probe method.

The pump-type actuators were prepared as following: Polytetrafluoroethylene (PTFE) boxes (length × width × depth is 15 × 15 × 10 mm) with one end open were firstly machined, and then carbon material films were glued onto the top of the boxes to seal the air inside. Two pieces of copper conductive strips were pasted on the films as electrodes. The electrical power was supplied by a Tektronix Arbitrary Function Generator (AFG3011), and the displacement was measured using a LK-G5001 laser displacement sensor. The laser was concentrated on the centre of the carbon material films to detect the displacement change. The temperature of the materials when the actuation deformation reached maximum during the actuation process was measured using a laser sight infrared thermometer with a resolution of 0.1 °C.

Results and discussion

Figure 1a shows the schematic drawing of the air pump-type electrothermal actuator we designed, in which various nanostructured carbon materials films were utilized as heating elements. When a driving voltage is applied, an electric current immediately flows through the film, and the heat generated due to Joule heating leads to expansion of the sealed air. Subsequently,



Figure 2 Digital images of as-prepared SWCNT, GO, *r*-GO and GO/SWCNT hybrid films

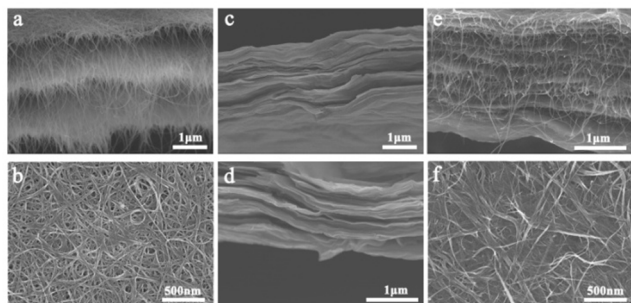


Figure 3 SEM images of (a, b) cross-sectional and top view of the SWCNT film; (c, d) cross-sectional view of the *r*-GO and the GO film; (e, f) cross-sectional and top view of the GO/SWCNT hybrid film.

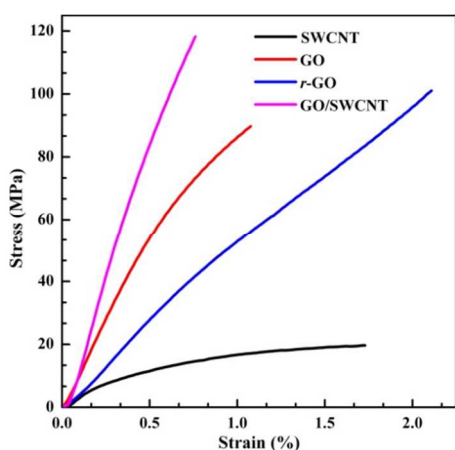


Figure 4 Typical stress-strain curves of as-prepared SWCNT, GO, *r*-GO and GO/SWCNT films.

the film would be plumped up, and reach the maximum deformation. Once the voltage is cut off, the heat generation is stopped immediately, and the film would recover to initial state accompanying by the air contraction. In general, the heat generated by carbon material film at a given time period greatly depends on driving voltages, electrical conductivity, and sample size.¹⁵ The thermal energy generated would enhance greatly with increasing driving voltages and electrical conductivity of materials, and eventually lead to effective air expansion. Moreover, considering the air expansion dominated actuation mechanism of our air pump-type actuator, the carbon material films with better gas-barrier property would efficiently hinder air permeation and leakage during the actuation process, and result in improved actuation stroke. Earlier works have proven that individual graphene sheets and its nanocomposites behaved good gas-impermeability due to its planar feature.^{16-18, 26} Meanwhile, the air volume sealed inside box also would affect the actuator performance at a given driving voltage. The air with small

volume could be expanded more effectively, and eventually lead to large actuator stroke. However, it is not under consideration in this work. Herein, the boxes were machined with the same dimensions to make the air volume influence on the actuation performance negligible.

In this work, GO and SWCNT were used as building blocks to fabricate various nanostructured carbon material films. All films were prepared via an environmental friendly method called vacuum-assisted self-assembly filtration we used before.²⁴ To illustrate the influence of various carbon material film microstructures on the actuation performance, herein, three kinds of carbon material films were prepared in the lab including SWCNT, *r*-GO and GO/SWCNT hybrid films. For comparison, the thickness of all the films was controlled in the range of 1.5-3.0 μm . Figure 2 shows digital images of the as-prepared SWCNT, *r*-GO, GO/SWCNT hybrid films with the diameter of about 40 mm. Four-probe electrical test indicated that the conductivities of SWCNT, *r*-GO, GO/SWCNT films were 120, 80 and 75 S/cm, respectively.

Figure 3a and 3b show SEM cross-sectional and top view of the as-prepared SWCNT film. The film has a laminar structure with entangled nanotubes to form network structure through van der Waals forces at tube-tube junctions, which would endow the film high electrical conductivity as well as mesoporous microstructures. The presence of mesoporous microstructure of SWCNT enables the electrolyte infiltrate efficiently during charge and discharge process, which eventually lead to enhanced actuation performance for ionic-type actuator.²⁷ However, on the other hand, the presence of mesopores in SWCNT film would greatly deteriorate actuation performance of air pump-type actuator due to air diffusion. Comparatively, Figure 3c shows that GO platelets were alternatively piled up to form a uniform layered structure, which was consistent with our previous work.²⁴ Such well-packed layered microstructure was still maintained after further chemical reduction (Figure 3d). Figure 3e presents the cross-sectional view of layered GO/SWCNT hybrid film. Earlier work has pointed out the presence of nanotubes will not greatly influence the self-assembly process of GO individual platelets during the vacuum-assisted filtration process. The main reason is due to the attachment of CNT onto GO platelets through π - π stacking interaction between the delocalized electrons in the aromatic regions of GO sheets and CNT in the mixed suspensions.²⁸ Different from the mesoporous structures of the SWCNT film, no apparent mesopores were observed in the hybrid films as shown in Figure 3f. Consequently, the highly dense packing feature of the *r*-GO and GO/SWCNT hybrid film together with perfect gas-impermeable nature of individual graphene and GO nanosheets are expected to exhibit excellent actuation performance.

For conventional EAP materials, the force generation is greatly limited by the modulus of actuator materials. Many studies have shown that the maximum stress that can be sustained by conventional EAPs during actuation appeared to be less than 10 MPa.^{8, 29, 30} Additionally, the low stress generation from conductive polymers implies that the application of mechanical amplifiers is also very limited. Alternatively, graphene and its hybrid films have shown superior mechanical properties, which show great potential in these fields. Figure 4 shows the typical

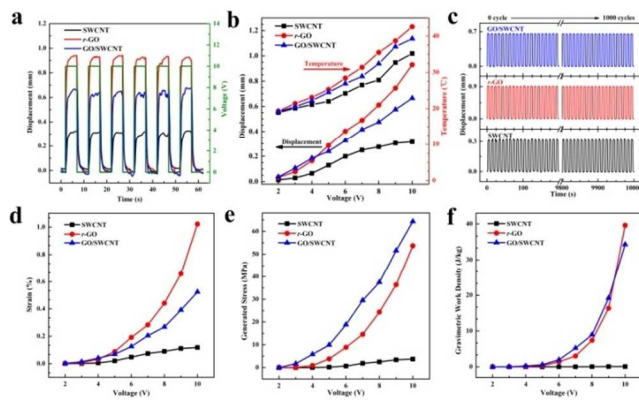


Figure 5 (a) Actuation displacement of pump actuators under 10V driving voltage; (b) working temperature and displacement as a function of driving voltage; (c) cyclic actuation performance; (d) actuation strain; (e) generated stress and (f) gravimetric work density

tensile stress-strain curves of carbon material films. Briefly speaking, the average tensile modulus and strength of various carbon material films are much higher than that of conducting polymers. Tensile tests indicated that modulus was 3.2 ± 0.45 GPa and 6.0 ± 0.53 GPa for SWCNT and *r*-GO films, respectively. After combination GO platelets with SWCNT, the modulus of hybrid film was increased from initial 10.6 ± 0.95 GPa for GO film to 15.2 ± 0.34 GPa, demonstrated an improvement about 40%. Theoretical simulations based on first-principles calculation have demonstrated that there are two major factors to determine the overall mechanical properties of GO film, namely inter-layer and intra-layer interaction.³¹ Herein, we speculate that the mechanical enhancement of the hybrid film may result from the increased intra-layer interaction, in which SWCNT with large aspect ratio on the order of 10^3 could easily intra-link adjacent GO sheets during the vacuum-assisted filtration process. Consequently, the increased intra-layer integration of GO platelets would benefit effectively load transfer along the in-plane direction, and then the tensile modulus was improved. In addition, considering the fact that both output stress and work density of actuators greatly depend on the modulus of actuator materials, therefore, the improvement of actuation performances are expected for the GO/SWCNT hybrid films. We will discuss it later.

The actuation performances of various carbon material films were tested under various square wave potential with frequency of 0.1 Hz. Figure 5a shows the actuation displacement of three actuators under a 10 V driving voltage. As seen, the films were promptly plumped up as the voltage was applied, and the deformation would be kept steadily during the electric stimulation process, which indicates the equilibrium between heat generation and dissipation. Once the voltage was cut off, the film would simultaneously recover to its original state. Among the three actuator materials, *r*-GO film showed the highest deformation up to 0.93 mm, whereas the values for GO/SWCNT and SWCNT films were 0.68 mm and 0.32 mm, respectively. Figure 5b summarized the actuation displacement and working temperature of the nanostructured carbon material films during the actuation process as a function of driving voltage. Upon increasing the driving voltages, larger electric currents flowed through carbon material films, and then more thermal energy could be generated

to induce air expansion efficiently. Consequently, the actuation displacement and working temperature would exhibit monotonically increasing trend with driving voltages prior to the structural failure of actuator films. For instance, the working temperature for the *r*-GO, GO/SWCNT and SWCNT films under 10 V driving voltage was 42.6, 39.3, and 35.2 °C, respectively. Among three actuator films, the *r*-GO film behaved the largest displacement as well as highest temperature at a given driving voltage. The repeatability and stability of the actuators were investigated by cyclic actuation under 10 V driving voltage as shown in Figure 5c. It is found that, the displacement could be maintained during the cyclic actuation process for more than 1000 cycles, indicating the long time working life of nanostructured carbon materials based pump actuators.

To quantitatively define the actuator strain, the plumped film is simplified as a dome once the deformation of the film reached maximum, as presented in Figure 1b. The actuation strain ϵ can be calculated by Equation 1, in which d stands for half length of the film, and δ represents the actuation displacement of the film from the initial state.

$$\epsilon = \frac{(d^2 + \delta^2) [\tan^{-1}(\frac{2d\delta}{d^2 - \delta^2})]}{2d\delta} - 1 \quad \text{Equation 1}$$

Figure 5d summarizes the derived actuation strain of the actuators as a function of applied voltages. It can be clearly seen that the strain show apparently increasing trend with driving voltages. Among three carbon material films, the *r*-GO film behaves the largest strain, whereas the SWCNT film possesses the smallest one within the whole driving voltage range. Specifically, the actuation strain of the *r*-GO film was about 1.02% at a 10 V driving voltage, which is approximately one order of magnitude higher than that of the SWCNT film (0.12%), and actuation strain of the GO/SWCNT film is located in the middle (0.52%).

As known, the magnitude of actuation stroke is mainly determined by the thermal energy generated and mechanical properties of actuator materials. Material with higher electrical conductivity would generate more heat according to Joule effect, and materials with lower modulus would be deformed much more easily. Thus, SWCNT film with highest electrical conductivity (120 S/cm) and lowest tensile modulus (3 GPa) is speculated to perform largest actuation displacement and strain among three carbon material films. However, experimentally, SWCNT film actuator exhibited smallest actuation displacement and strain under various driving voltages. This phenomenon should be attributed to the presence of mesoporous microstructure of the SWCNT films as presented in Figure 3b, in which air leakage easily occurred during electrical stimulus process. Thus, the efficient heat dissipation led to the relative low working temperature for SWCNT film as presented in Figure 5b. Conversely, the excellent gas-impermeability of *r*-GO platelets efficiently hindered the air diffusion during the actuation process and thereby the *r*-GO film exhibited largest actuation deformation. In addition, compare to maximum displacement of the CNT/PDMS nanocomposite (~1.1 cm at 10 V), the displacement amplitudes of the *r*-GO actuator showed the same level under a 10 V stimulus.^{12, 14} But, larger output force is expected for the *r*-GO actuators due to higher modulus on the level of GPa versus that of MPa for CNTs/PDMS nanocomposites. Given that

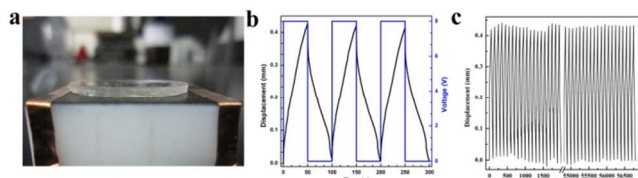


Figure 6 (a) Optical image of the weight-lifting test of GO/SWCNT hybrid film actuator; (b) actuation displacement under 8 V driving voltage with 300 times higher load; (c) cyclic weight-lifting actuation performance.

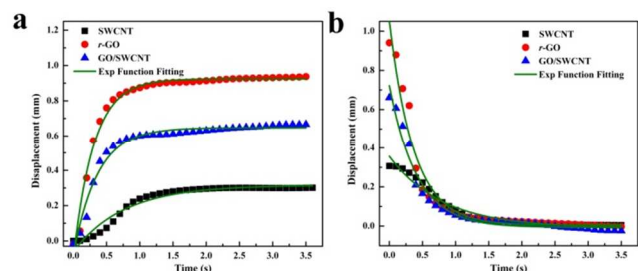


Figure 7 (a) Response time and (b) recovery time fitting for carbon material film actuators

Table 1 Response and recovery fitting results under 10V driving voltage

Actuator Materials	Response Time (ms)	Recovery Time (ms)
SWCNT	764	795
r-GO	308	370
GO/SWCNT	364	414
CNT/polymer (30 V DC voltage) ¹²	about 20s	about 50s

actuation strain of tested actuator materials within elastic deformation range, the generated stress of actuator at given driving voltages could be further derived from the typical tensile stress-strain curves of the carbon material films (Figure 4). Figure 5e presents the generated stress as a function of applied voltage. Specifically, at a 10 V driving voltage, the generated stress for SWCNT, r-GO and GO/SWCNT films were 3.75 MPa, 53.7 MPa and 64.3 MPa respectively. Comparatively, the generated stress of the hybrid film is at least two orders of magnitude higher than that of CNTs/PDMS nanocomposites at 52 V.¹⁴ Even though the actuation strain of the GO/SWCNT hybrid film was smaller than that of r-GO film, the relatively higher modulus rendered the hybrid film generate larger stress. To further examine the weight-lifting performance of the actuator, a piece of PDMS film (280 mg) which is about 300 times heavier than the weight of the GO/SWCNT film was placed onto the top of actuator, as shown in Figure 6a. It is found that the PDMS film could be lifted upward when a driving voltage was applied (a movie showing the actuation process can be available in the supporting information). Figure 6b shows the actuation displacement at 8 V driving voltage with frequency of 0.01 Hz. It was found that actuation displacement (0.425 mm) could be approximately same as the load-free actuation displacement (0.475 mm), which confirms the excellent stress output property of the GO/SWCNT actuator. It should also be noticed that, compared with the actuation process

without load, it would take much more time to reach the maximum displacement due to the weight lifting. Once the driving voltage was cut off, the heat generation would be stopped simultaneously. Subsequently, the actuator film was slowly recovered to its initial state. Such retardance of the displacement was attributed to the impeded heat dissipation induced by PDMS, thus much more time was required to get recovery. The cyclic experiment was carried out to examine the working life of the actuators under loading condition. It is found that, after long time cyclic actuation, the actuation performance was still maintained (as shown in Figure 6c), which implied the excellent loading capability of the actuator.

With the assumption that the plumped film underwent a uniform plane stress state as described in Figure 1c, the gravimetric work density (P) could be obtained by Equation 2, in which E and ν means the Young's modulus and Poisson's ratio of the materials respectively, and ρ is the mass density of the materials.

$$P = \left(\frac{E}{1-\nu} \right) \epsilon^2 \quad \text{Equation 2}$$

The gravimetric work density of actuators derived from Equation 2 show monotonic enhancement with increasing driving voltage, as presented in Figure 5f. Comparatively, the enhanced trend of r-GO and GO/SWCNT actuators is much more significant than that of the SWCNT actuator. Specifically, the gravimetric work density for r-GO and GO/SWCNT actuators was 39.6 and 34.3 J/kg respectively at 10 V, which is more than 500 times higher than that of SWCNT actuator (0.06 J/kg). Such significant improvement could be attributed to both the larger actuation strain and higher modulus of the r-GO and the GO/SWCNT films. Earlier work done by Baughman et al has shown a large work capacity (30 J/kg) obtained for CNT aerogel sheets actuated under 1.6 kV driving voltage.³² Herein, a much lower driving voltage (10 V) was required to achieve the comparable work density by using r-GO or GO/SWCNT film based pump-type electrothermal actuators.

Apart from the actuation strain, generated stress and gravimetric work density as discussed above, the response time is another important parameter to evaluate the actuator performances. Herein, the response and recovery time of the actuators were derived using curve fitting based on the following equations:

$$\delta(t) = \delta_0(1 - e^{-\frac{t}{t_0}}) \quad \text{Equation 3}$$

$$\delta(t) = \delta_1 + \delta_0 e^{-\frac{t}{t_1}} \quad \text{Equation 4}$$

In the equations, δ represents actuation displacement at time t , δ_0 relates to maximum actuation displacement, and δ_1 is residual actuation displacement during recovery process, t_0 and t_1 stand for response and recovery time respectively. Figure 7a and b present the curve fitting results of different actuator materials at a 10 V driving voltage. It can be clearly seen that the Eq. 3 and Eq. 4 fitted well with the response and recovery curves. The response and recovery time of r-GO, SWCNT and GO/SWCNT actuators are summarized in Table 1. Apparently, the response and recovery time of all actuator materials are within the range of few hundreds of ms, which is at least one order of magnitude shorter than that of the CNT/polymer nanocomposites electrothermal actuators (response time ranged from few seconds to several tens of seconds).¹² According to previous study, the quality factor,

$C_p\rho/\sigma$, was proposed to define the speed with which a material can be heated via an electric current, where C_p , ρ and σ are the material's specific heat capacity, density and electrical conductivity, respectively. A low quality factor implies that the material will heat more rapidly under an applied voltage.¹⁵ In our case, the electrical conductivity of the actuator materials is in the range of 70- 120 S/cm, which are at least two orders of magnitude higher than that of polymer nanocomposites. The quick response of our pump actuator could be attributed to the high electrical conductivity of carbon material films. Once the voltage was turned on, the films would be heated spontaneously and the air would be expanded promptly. On the other hand, once the voltage was turned off, the thermal energy generation via Joule heating stop immediately, and then the air would contract to initial state. Specifically, the *r*-GO film actuator behaved the fastest response and recovery speed among three actuators, while the GO/SWCNT turned to be slightly slower, and the SWCNT actuator performed the longest response and recovery time. The observed difference in response and recovery time could be attributed to the variation in microstructures of actuator materials. The excellent response and recovery behaviors of the *r*-GO and GO/SWCNT film actuators are originated from the gas-impermeability of graphene and GO nanosheets. On the other hand, the SWCNT film actuator with mesoporous structures would take much more time to achieve the maximum deformation because of air permeation. Meanwhile, for a given actuator, the recovery time is quite close to response time, further indicating good operation stability and reproducibility of the pump-type actuators.

Conclusion

In summary, we designed and fabricated electrothermal air pump-type actuators by utilization of SWCNT, *r*-GO, GO/SWCNT as heating elements and mechanical force generator. Compared with common polymer nanocomposites electrothermal actuators, air pump-type actuators performed better actuation performance as well as longer service life. Specifically, under a 10V driving voltage, the generated stress and work density could reach more than 50 MPa and 30 J/kg for the GO/SWCNT hybrid film actuator. The actuator performed excellent weight-lifting behaviour and stroke consistence with an external load which was about 300 times heavier than the weight of actuator film, and demonstrated excellent loading capability for long time cyclic actuation process. The response and recovery time of carbon material actuators are on the level of few hundreds of ms, at least one order of magnitude faster than that of electrothermal polymer nanocomposite actuators. The large generated stress together with rapid response at low driving voltage enable this type of actuator potentially applied in various aspects, such as sensor, switches, biomimetic breath equipment, and so on.

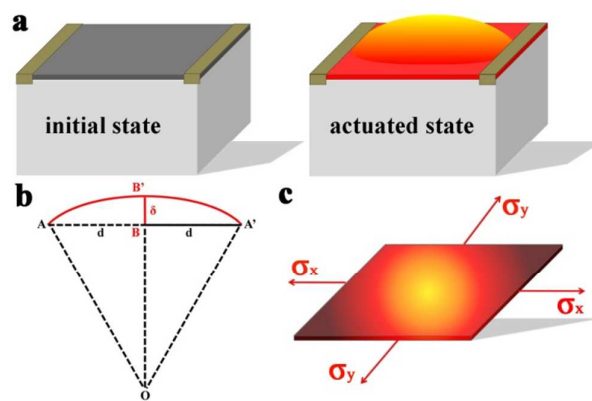
Acknowledgement

This project was jointly supported by the National Key Basic Research Program of China (Grant Nos. 2012CB937503 and 2013CB934203) and the National Natural Science Foundation of China (Grant Nos. 51173030 and 11225210).

Notes and references

- ^a National Center for Nanoscience and Technology, Beijing, P. R. China, 100190, Fax: +86-10-8254-5586; Tel: +86-10-8254-5586; E-mail: zhong.zhang@nanoctr.cn
- ^a National Center for Nanoscience and Technology, Beijing, P. R. China, 100190, Fax: +86-10-6265-6765; Tel: +86-10-8254-5587; E-mail: liulq@nanoctr.cn
- ^b University of Chinese Academy of Science, Beijing, China, 100049
- † Electronic Supplementary Information (ESI) available: A movie showing the weight-lifting actuation process of GO/SWCNT actuator. See DOI: 10.1039/b000000x/
- S. Maeda, Y. Hara, T. Sakai, R. Yoshida and S. Hashimoto, *Adv. Mater.*, 2007, **19**, 3480.
 - T. Mirfakhrai, J. Madden and R. Baughman, *Materialstoday*, 2007, **10**, 30.
 - K. Cho, J. Rosmarin and H. Asada, IEEE International Conference on Robotics and Automation, 2007, 921.
 - E. Smela, *Adv. Mater.*, 2003, **15**, 481.
 - H. Jiang, S. Kelch and A. Lendlein, *Adv. Mater.*, 2006, **18**, 1471.
 - M. Shahinpoor and K. J. Kim, *Smart. Mater. Struct.*, 2001, **10**, 819.
 - S. D. Deshpande, J. Kim and S. R. Yun, *Smart. Mater. Struct.*, 2005, **14**, 876.
 - R. Pelrine, R. Kornbluh, Q. Pei and J. Joseph, *Science*, 2000, **287**, 836.
 - R. Shankar, T. K. Ghosh and R. J. Spontak, *Adv. Mater.*, 2007, **19**, 2218.
 - S. Zhang, N. Zhang, C. Huang, K. Ren and Q. Zhang, *Adv. Mater.*, 2005, **17**, 1897.
 - C. Park, J. H. Kang, J. S. Harrison, R. C. Costen and S. E. Lowther, *Adv. Mater.*, 2008, **20**, 2074.
 - Y. Hu, G. Wang, X. Tao and W. Chen, *Macromol. Chem. Phys.*, 2011, **212**, 1671.
 - M. Kato and M. Ishibashi, *J. Phys.: Conf. Ser.*, 2008, **127**, 012003.
 - L. Z. Chen, C. H. Liu, C. H. Hu and S. S. Fan, *Appl. Phys. Lett.*, 2008, **92**, 263104.
 - A. T. Sellinger, D. H. Wang, L. S. Tan and R. A. Vaia, *Adv. Mater.*, 2010, **22**, 3430.
 - O. Leenaerts, B. Partoens and F. M. Peeters, *Appl. Phys. Lett.*, 2008, **93**, 193107.
 - J. S. Bunch, S. S. Verbridge, J. S. Alden, A. M. van der Zande, J. M. Parpia, H. G. Craighead and P. L. McEuen, *Nano Lett.*, 2008, **8**, 2458.
 - R. R. Nair, H. A. Wu, P. N. Jayaram, I. V. Grigorieva and A. K. Geim, *Science*, 2012, **335**, 442.
 - R. H. Baughman, A. A. Zakhidov and W. A. de Heer, *Science*, 2002, **297**, 787.
 - Y. Zhu, S. Murali, W. Cai, X. Li, J. W. Suk, J. R. Potts and R. S. Ruoff, *Adv. Mater.*, 2010, **22**, 3906.
 - H. Chen, M. B. Müller, K. J. Gilmore, G. G. Wallace and D. Li, *Adv. Mater.*, 2008, **20**, 3557.
 - L. Wang, C. Li, D. Wang, Z. Dong, F. X. Zhang and J. Jin, *J. Nanosci. Nanotechnol.*, 2013, **13**, 5461.
 - S. E. Zhu, R. Shabani, J. Rho, Y. Kim, B. H. Hong, J. H. Ahn and H. J. Cho, *Nano Lett.*, 2011, **11**, 977.
 - Y. Gao, L.-Q. Liu, S.-Z. Zu, K. Peng, D. Zhou, B.-H. Han and Z. Zhang, *ACS NANO*, 2011, **5**, 2134-2141.
 - S. Pei, J. Zhao, J. Du, W. Ren and H.-M. Cheng, *Carbon*, 2010, **48**, 4466.
 - O. C. Compton, S. Kim, C. Pierre, J. M. Torkelson and S. T. Nguyen, *Adv. Mater.*, 2010, **22**, 4759.
 - R. H. Baughman, C. Cui, A. A. Zakhidov, Z. Iqbal, J. N. Barisci, G. M. Spinks, G. G. W. A. Mazzoldi, D. D. Rossi, A. G. Rinzler, O. J. S. Roth and M. Kertesz, *Science*, 1999, **284**, 1340.
 - L. Qiu, X. Yang, X. Gou, W. Yang, Z. F. Ma, G. G. Wallace and D. Li, *Chem. Eur. J.*, 2010, **16**, 10653.
 - A. Mazzoldi, C. Degl'Innocenti, M. Michelucci and D. De Rossi, *Mater. Sci. Eng. C*, 1998, **6**, 65.

-
30. A. S. Hutchison, T. W. Lewis, S. E. Moulton, G. M. Spinks and G. G. Wallace, *Synthetic Metals*, 2000, **113**, 121.
 31. Y. Liu, B. Xie and Z. Xu, *J. Mater. Chem.*, 2011, **21**, 6707.
 32. A. E. Aliev, J. Oh, M. E. Kozlov, A. A. Kuznetsov, S. Fang, A. F. Fonseca, R. Ovalle, M. D. Lima, M. H. Haque, Y. N. Gartstein, M. Zhang, A. A. Zakhidov and R. H. Baughman, *Science*, 2009, **323**, 1575.



We fabricate electrothermal air pump-type actuators by utilization of SWCNT, *r*-GO, GO/SWCNT as heating elements and mechanical force generator.